Differential viral RNA methylation contributes to pathogen blocking in *Wolbachia*-colonized arthropod

Tamanash Bhattacharya[1‡], Liewei Yan[2], Hani Zaher[2] Irene L.G. Newton[1*], Richard W. Hardy[1*]

[1]Department of Biology, Indiana University, Bloomington, Indiana, United States of America

[2]Department of Biology, Washington University, St. Louis, Missouri, United States of America

[‡]current address: Basic Sciences Division, Fred Hutchinson Cancer Research Center, Seattle, Washington, United States of America

*Corresponding authors: ILGN, RWH

Email: irnewton@indiana.edu, rwhardy@indiana.edu

Tamanash Bhattacharya: 0000-0002-8129-7568

Irene L.G. Newton: 0000-0002-7118-0374

Richard W. Hardy: 0000-0001-6912-6291

Keywords

Virus, Mosquito, *Wolbachia*, Nanopore, Methylation

Abstract

Arthropod endosymbiont *Wolbachia pipientis* is part of a global biocontrol strategy aimed at reducing the spread of mosquito-borne RNA viruses such as alphaviruses. Our prior work examining *Wolbachia*-mediated pathogen blocking has demonstrated (i) the importance of a host cytosine methyltransferase, DNMT2, in *Drosophila*, and (ii) viral RNA as a target through which pathogen-blocking is mediated. Here we report on the role of DNMT2 in *Wolbachia* induced virus inhibition of alphaviruses in *Aedes sp..* Mosquito DNMT2 levels were altered in the presence of both viruses and *Wolbachia,* albeit in opposite directions. Elevated levels of DNMT2 in mosquito salivary glands induced by virus infection were suppressed in *Wolbachia* colonized animals coincident with a reduction of virus replication, and decreased infectivity of progeny virus. Ectopic expression of DNMT2 in cultured *Aedes* cells was proviral increasing progeny virus infectivity, and this effect of DNMT2 on virus replication and infectivity was dependent on its methyltransferase activity. Finally, examination of the effects of *Wolbachia* on modifications of viral RNA by LC-MS showed a decrease in the amount of 5-methylcytosine modification consistent with the down-regulation of DNMT2 in *Wolbachia* colonized mosquito cells and animals. Collectively, our findings support the conclusion that disruption of 5-methylcytosine modification of viral RNA is an important mechanism operative in pathogen blocking. These data also emphasize the essential role of epitranscriptomic modifications in regulating fundamental processes of virus replication and transmission.

Significance Statement

Presence of the endosymbiont *Wolbachia pipientis* in the arthropod host reduces establishment and dissemination of several emerging arboviruses within the insect and prevents virus transmission to a vertebrate host. However, the precise mechanisms mediating this inhibition are unknown. In this study, we demonstrate that the host RNA cytosine methyltransferase DNMT2 is an important regulator of this process. Our findings establish DNMT2 as a host factor targeting the viral RNA and as a conserved determinant of *Wolbachia*-mediated pathogen blocking. Importantly, we reveal a previously understudied role of virion encapsidated RNA methylation in regulating alphavirus particle infectivity in naïve cells.

Introduction

Viruses are remarkably adept at using a limited set of viral factors to replicate in vastly different host cell environments. This ability is vital for the success of arboviruses, which encounter physiologically and ecologically distinct invertebrate and vertebrate hosts during transmission. As these viruses oscillate between vertebrate and arthropod hosts, the progeny virions reared in one host cell context are primed for the next. Indeed, differences in the infectivity of arboviruses derived from invertebrate and vertebrate cells supports the idea of host-specific adaptations (1, 2). In the case of alphaviruses in particular, viruses derived from mosquito cells are more infectious on vertebrate cells on a per-particle basis relative to vertebrate cell-derived viruses and vice versa. Indeed, a subset of the total virus populations derived from vertebrate cell cultures are better at establishing infection in mosquito midguts following blood-meal (1). Remarkably, infectivity of these viruses resembles those isolated from serum of virus-infected mice, which represent the natural source of viruses that establish midgut infection in mosquitoes. This carries the implication that progeny viruses originating from one cell type may possess intrinsic properties that can confer a fitness advantage while infecting a destination host cell type, altering their

infectivity on these destination cells on a per-particle level. As to what such properties may represent, current evidence points towards differences in virus structure, like differential sialation or glycosylation of viral glycoproteins impacting host receptor-binding and/or differences in the encapsidated cargo e.g., packaging of host ribosomal components (2-4). Another property that might confer unique cell type-specific advantages to viruses is differential modification of the virion RNA. Indeed, recent evidence shows that modifications like N^6-methyladenosine (m6A) and 5-methylcytosine (m5C) can regulate viral RNA functionality in the cell (5, 6). Therefore, it is possible that such modifications also influence infectivity of progeny viruses produced from said cells.

One variable that alters the ability of viruses to replicate within arthropod cells is the presence of the endosymbiont *Wolbachia pipientis.* The symbiont alters the host cell environment such that it becomes refractory to +ssRNA viruses (7-10). We recently reported that presence of *Wolbachia* in mosquitoes also results in reduced infectivity of progeny viruses, consequently limiting virus dissemination within the mosquito and consequently transmission into naïve vertebrate cells (11). We have also shown that the viral RNA is a cellular target of *Wolbachia*-mediated inhibition and that loss in progeny virus infectivity occurs at the level of the encapsidated virion RNA, which is compromised in ability to replicate in naïve vertebrate cells (11). Based on these results, we therefore speculated that factor(s) regulating pathogen blocking likely target the viral plus sense RNA genome, a feature shared between all viruses susceptible to *Wolbachia*-mediated inhibition. Indeed, in an earlier study we identified the RNA cytosine methyltransferase (MTase) gene DNMT2 as a host determinant of pathogen blocking in fruit flies (9). DNMT2 is a RNA cytosine MTase that functions as a m5C writer to cellular RNA substrates like transfer RNA species, protecting them from stress-induced degradation (12). In the process, it has also been shown to contribute to efficient functioning of Dicer-2 in the fruit fly (13). Past studies in this system have also demonstrated DNMT2's role in retrotransposon silencing, as a general immune modulator that confers host protection against pathogenic bacteria and as an antiviral against RNA viruses native to the fly host (13-15). Loss of DNMT2 in *w*Mel-colonized flies increased Sindbis virus RNA and protein synthesis and ultimately, infectious virus output, implying an antiviral role of this RNA MTase in pathogen blocking in *Drosophila melanogaster* (9).

Here, we investigate whether DNMT2 is important for *Wolbachia*-mediated pathogen blocking in mosquitoes. Additionally, we ask whether this MTase is functionally important for virus regulation in the absence of *Wolbachia.* Given DNMT2's biological role as a cellular RNA cytosine methyltransferase, we further interrogate the possibility of m5C modification of viral RNA in mosquito cells and whether viral RNA is differentially modified in the presence and absence of *Wolbachia* in mosquito cells. We find that *Wolbachia* and viruses differentially influence MTase expression in mosquitoes. Specifically, presence of virus lead to elevated MTase expression, which is proviral in mosquito cells. In contrast, presence of *Wolbachia* downregulates MTase levels to seemingly disrupt this proviral state, contributing to virus inhibition as well as reduced progeny virus infectivity. The proviral effect is dependent on the catalytic activity of DNMT2. Finally, as a consequence of this downregulation and DNMT2's role as a RNA cytosine MTase, we show that the presence of *Wolbachia* in cells result in reduced abundance of 5-methylcytosine (m5C) modification of progeny viral RNA. These changes imply that m5C modifications play a role in regulating viral RNA infectivity in mammalian cells. In summary, our findings highlight a previously underappreciated role of RNA methylation in alphavirus dissemination and transmission. Overall, our results indicate a role of the viral epitranscriptome as regulatory signatures capable of influencing the transmission of other arboviruses.

Results

Virus and *Wolbachia* differentially modulate *Aedes* DNMT2 expression

The presence of *Wolbachia* in dipterans alter the expression of DNMT2. In adult female *Drosophila melanogaster* (9), *Wolbachia* elevates DNMT2 (*Mt2*) expression. In contrast, *Wolbachia* in *Aedes* mosquitoes are associated with reduced DNMT2 (*AMt2*) expression (16). However, in both cases, these conditions of altered DNMT2 expression are accompanied by efficient RNA virus restriction, which prompted us to investigate the regulatory role of this MTase in arbovirus replication both within and outside of the context of *Wolbachia* infection. To this end, we first examined the expression of *AMt2* in *w*AlbB-colonized *Aedes aegypti* mosquitoes. We chose to assess *in vivo AMt2* expression changes in two ways: Given that our recent study implied losses in RNA virus dissemination in *Wolbachia*-colonized mosquito cells, we first asked whether MTase expression is altered in whole mosquito tissues (Fig 1A). Second, given their direct role in producing progeny viruses that undergo transmission to vertebrate hosts, we also assessed *AMt2* expression in isolated salivary gland tissues (Fig 1A-B).

AMt2 expression was measured in five-day old female *Aedes aegypti* mosquitoes colonized with and without *Wolbachia (w*AlbB), following bloodmeals with and without Sindbis virus (SINV) (Fig 1B). Presence of both endosymbiont and virus was associated with altered *AMt2* expression (Two-way ANOVA, $p < 0.0001$), with elevated *AMt2* levels in *Wolbachia*-free mosquitoes that received an infectious, virus containing bloodmeal (Fig 1B. W-/V- compared to W-/V+; Two-way ANOVA, $p < 0.0001$). In contrast, we found *Wolbachia* to reduce *AMt2* expression in mock infected individuals (W+/V-) (Fig 1B. W-/V- compared to W+/V-; Two-way ANOVA, $p = 0.0037$). Importantly, *AMt2* expression was also reduced in *Wolbachia*-colonized mosquitoes post infectious (V+) bloodmeal, indicating that during *Wolbachia*-mediated pathogen blocking, virus replication occurs under low *AMt2* expression (Fig 1B. W-/V- compared to W+/V+; Two-way ANOVA, $p = 0.0054$). This pattern of reduced *AMt2* expression was also observed *ex vivo* in cultured *Aedes albopictus* -derived mosquito (RML12) cells colonized with both a native (*w*AlbB strain in Aa23 cells) and a non-native *Wolbachia* (*w*Mel in RML12 cells) strain; Unpaired Mann Whitney U-tests: RML12-*w*Mel – $p = 0.0028$, Aa23-*w*AlbB – $p = 0.0286$ (Fig S1).

We next quantified *AMt2* expression in isolated salivary gland tissues from five-day old *Aedes aegypti* mosquitoes colonized with or *Wolbachia*-free *(w*AlbB), post bloodmeal with (V+) or without (V-) SINV (Fig 1C). Overall expression patterns of *AMt2* in the salivary gland tissues were similar to that observed across whole mosquitoes, (Fig 1C. W-/V- compared to W-/V+; Two-way ANOVA, $p < 0.0001$). As before, presence of *Wolbachia* alone was associated with lower *AMt2* expression, albeit the difference was not statistically significant (Fig 1C. W-/V- compared to W+/V-; Two-way ANOVA, $p = 0.1064$). Importantly however, *Wolbachia* did prevent SINV-induced *AMt2* upregulation, reducing it by two-three-fold (Fig 1C. W-/V+ compared to W+/V+; Two-way ANOVA, $p = 0.0027$). Under these conditions, we also observed a significant reduction in viral RNA in the salivary gland tissues; Welch-corrected unpaired t-test, $p < 0.0001$, $t = 10.37$, $df = 8.839$ (Fig 1D). It should be noted that our observations regarding the effect of *Wolbachia* (*w*AlbB) or SINV on *AMt2* expression are analogous to previous reports that describe differential *AMt2* expression in the presence of the flavivirus DENV-2 and *Wolbachia* (*w*Mel) in *Aedes aegypti* mosquitoes (16). All together, these observations suggest that in contrast to *Drosophila melanogaster*, presence of *Wolbachia* in *Aedes* mosquitoes is associated with reduced host MTase expression (9).

DNMT2 promotes virus infection in mosquito cells

159 The positive correlation between *AMt2* expression and SINV genome replication in *Aedes*
160 mosquitoes (Fig 1B-D) led us to examine whether there is a functional consequence of elevated
161 MTase expression on virus infection in these insects. We therefore ectopically expressed *AMt2*
162 and assessed its effect on virus infection in cultured *Aedes albopictus* cells (Fig 2A), starting with
163 azacytidine-immunoprecipitation (AZA-IP) to determine whether viral RNA in the cell is a direct
164 DNMT2 target. *Wolbachia*-free *Aedes albopictus* (C7-10) cells were transfected with an epitope-
165 tagged *AMt2* expression vector (FLAG-*AMt2*) or control vector (FLAG-empty) for 48 hours prior
166 to infection with SINV at an MOI of 10. After 24 hours post-infection, cells were labelled with a
167 cytosine analog, 5-Azacytidine (5-AZAC) for 18 hours to allow incorporation of the label into newly
168 synthesized cellular and viral RNA. We reasoned that if mosquito DNMT2 directly target viral
169 RNAs for methylation, the presence of 5-AZAC in the RNA should covalently trap the enzyme
170 forming a stable m5C-DNMT2-viral RNA complex, allowing co-immunoprecipitation of the RNA-
171 protein complexes using anti-FLAG antibody (17). Targeted quantitative RT-PCR analyses of total
172 immunoprecipitated RNA revealed an enrichment of SINV RNA relative to a control host RNA
173 transcript (GAPDH), confirming that viral RNA is indeed a direct MTase target in these cells;
174 Unpaired two-tailed t-test with Welch's correction, $p = 0.0004$, $t = 4.216$, $df = 20$ (Fig 2B).

175 We next assessed the effect of elevated *AMt2* expression on RNA virus infection by measuring
176 the output of infectious progeny viruses following infection into cells expressing FLAG-*AMt2*.
177 Ectopic MTase expression resulted in a four-fold increase in SINV titer, further supporting the
178 positive *in vivo* correlation between *AMt2* expression and virus replication observed previously *in*
179 *vivo*; Unpaired two-tailed t-test with Welch's correction, $p = 0.0002$, $t = 5.404$, $df = 11.81$ (Fig 2C).
180 We also observed a concomitant increase in the per-particle infectivity of viruses upon assaying
181 them on vertebrate baby hamster kidney fibroblast cells, as evidenced by higher specific infectivity
182 ratios; Unpaired two-tailed t-test with Welch's correction, $p = 0.0084$, $t = 3.911$, $df = 5.820$ (Fig
183 2D). These data indicate that the increase in titer observed during elevated *AMt2* expression
184 levels is a consequence of increased particle infectivity rather than an increase in particle
185 production. Together these results support the idea of *Aedes* DNMT2 being a proviral factor that
186 is exploited by the virus to enhance its replication and transmission in the mosquito vector.

187 Given that *AMt2* expression is reduced in the presence of *Wolbachia,* we hypothesized that virus
188 restriction *in vivo* is a consequence of reduced DNMT2 levels. To test this, virus replication in
189 mosquito cells following pharmacological MTase inhibition was measured. Structural homology
190 of DNMT2 to other members of the DNA MTase family has allowed it to retain its DNA binding
191 ability *in vitro* although they are canonically known to methylate tRNA molecules (18). Therefore,
192 pretreatment of cells with either an ribo- (5-Azacytidine or 5-AZAC) or deoxyribo- (Deoxy-5-
193 Azacytidine or DAC5) MTase inhibitor should result in reduced cellular DNMT2 activity and
194 consequently restrict alphavirus replication. Pretreating *Wolbachia*-free C7-10 cells with RNA
195 MTase inhibitor 5-AZAC prior to infection reduced SINV RNA replication 24 hours post infection
196 at MOI=10; Unpaired two-tailed t-test with Welch's correction, SINV: $p = 0.0012$, $t = 6.742$, $df =$
197 4.892, (Fig S2A). Virus titers was also reduced approximately ten-fold; Unpaired two-tailed t-test
198 with Welch's correction, SINV: $p = 0.0339$, $t = 4.541$, $df = 2.322$ (Fig S2B). Finally, MTase inhibition
199 also negatively influenced SINV per-particle infectivity, as evidenced by a significantly reduced SI
200 ratio; Unpaired two-tailed t-test with Welch's correction, SINV: $p = 0.0002$, $t = 12.59$, $df = 3.946$
201 (Fig S2C). Similar results were obtained for related alphavirus, Chikungunya virus (CHIKV) 48
202 hours post infection at an MOI of 10; Unpaired two-tailed t-test with Welch's correction, CHIKV
203 viral RNA: $p < 0.0001$, $t = 35.30$, $df = 6.001$, CHIKV titer: $p = 0.0019$, $t = 4.864$ $df = 6.940$ (Fig
204 S3A,B). Using our previously published live-cell imaging system, we used a fluorescently-tagged
205 CHIKV reporter virus (CHIKV-mKate) to examine the effect of deoxyribo- MTase inhibitor DAC5
206 on virus replication in *Wolbachia*-free and *Wolbachia*-colonized *Aedes albopictus* cells using the

207 Incucyte live-cell imaging platform (11). As before, fluorescent protein expression was used as a
208 proxy of virus spread in cells with and without the inhibitor (DMSO) pretreatment, following
209 synchronized virus adsorption at 4ºC. Post adsorption, cell monolayers were extensively washed
210 with 1XPBS to remove any unbound viruses, followed by the addition of warm media to initialize
211 virus internalization and infection. Virus spread was measured over 50 hours by quantifying mean
212 virus-encoded red fluorescent reporter (mKate) expression observed over four distinct fields of
213 view taken per well every 2-hours (Fig S3C).

214 Viruses derived from *Wolbachia*-colonized cells (W+ virus) produced under low *AMt2* conditions
215 are less infectious on naïve cells which limit their dissemination to mosquito cells (11). Notably,
216 this phenotype is particularly pronounced when such viruses encounter cells also colonized with
217 the endosymbiont, which presumably also exhibit reduced *AMt2* expression (Fig S3D-E). We
218 therefore reasoned that replication kinetics of W+ viruses in inhibitor-treated *Wolbachia*-free (W-
219) cells should phenocopy kinetics of W+ virus spread in *Wolbachia*-colonized (W+) cells.
220 Additionally, kinetics of W- virus spread in inhibitor treated *Wolbachia*-free (W-) cells should
221 phenocopy W- virus spread in *Wolbachia*-colonized (W+) cells (11). Three-way ANOVA was used
222 to determine the effect of MTase inhibitor (DAC5), progeny virus type (derived from cells with or
223 *Wolbachia*-free*)* and/or time on virus spread in target cells (cells with or *Wolbachia*-free*)*. Below,
224 we refer to viruses derived from *Wolbachia*-colonized insect cells as W+ and their counterparts,
225 derived from *Wolbachia*-free cells as W-. Consistent with our previous report, spread of W+
226 viruses in mock treated control *Wolbachia*-free cells was significantly reduced relative to W-
227 viruses over time (11). In the presence of MTase inhibitor, spread of both W- and W+ viruses was
228 reduced over the course of infection, with a greater decrease in the replication of W+ viruses
229 relative to W- viruses, indeed phenocopying the spread of W+ viruses in *Wolbachia*-colonized
230 cells. Finally, replication of W- viruses in the presence of inhibitor was comparable to that of W+
231 viruses in mock-treated *Wolbachia*-free cells; Three-way ANOVA with Tukey's multivariate
232 analyses, DAC5: $p < 0.0001$, Virus Source: $p < 0.0001$, Time: $p < 0.0001$, DAC5 X Time: $p <$
233 0.0001, Source X Time: $p < 0.0001$, Virus Source X DAC5: $p = 0.1148$, Virus Source X DAC5 X
234 Time: $p > 0.999$ (Fig S3D). We observed no synergistic effect of virus source, and MTase inhibitor
235 on virus spread in target *Wolbachia*-colonized cells, likely as a consequence of low mean reporter
236 activity; Three-way ANOVA with Tukey's multivariate analyses, DAC5: $p = 0.1793$, Virus Source:
237 $p = 0.5060$, Time: $p < 0.0001$, DAC5 X Time: $p > 0.99$, Virus Source X Time: $p > 0.99$, Virus
238 Source X DAC5: $p = 0.1039$, Virus Source X DAC5 X Time: $p = 0.9804$ (Fig S3E).

239 **Ectopic DNMT2 expression rescue viruses from *Wolbachia*-mediated inhibition**

240 If *AMt2* downregulation is responsible for pathogen blocking in mosquitoes, ectopic *AMt2*
241 overexpression in *Wolbachia*-colonized mosquito cells should alleviate the virus inhibition
242 phenotype, which include disruption of viral RNA synthesis and progeny virus infectivity. Indeed,
243 consistent with this hypothesis, we observed a significant reduction in viral RNA levels in
244 *Wolbachia*-colonized cells relative to cells *Wolbachia*-free; One-way ANOVA Holm-Sidak's
245 multiple comparisons test, w/o Wolb vs w/ Wolb, $p < 0.0001$ (Fig 3A). Quantitative RT-PCR
246 analyses of SINV RNA showed increased viral RNA levels in *Wolbachia*-colonized cells
247 expressing FLAG-*AMt2* relative to cells carrying the control FLAG-empty vector, suggesting
248 restored virus RNA synthesis; One-way ANOVA Holm-Sidak's multiple comparisons test, w/ Wolb
249 vs w/ Wolb + AMt2, $p < 0.0001$ (Fig 3A). Additionally, we observed a significant improvement in
250 per-particle infectivity of progeny viruses derived from *Wolbachia*-colonized cells ectopically
251 expressing *AMt2* (W+ AMt2+ virus); One-way ANOVA Holm-Sidak's multiple comparisons test,
252 w/ Wolb vs w/ Wolb + AMt2, $p = 0.0003$, w/o Wolb vs w/ Wolb, $p < 0.0001$ (Fig 3B). Therefore,
253 both phenotypes of pathogen blocking were restored upon *AMt2* over-expression. Additionally,

254 we assessed whether ectopic *AMt2* expression alters *Wolbachia* titer in *Aedes albopictus* (C7-10)
255 cells. Given that endosymbiont titers can influence the degree of virus inhibition, we asked
256 whether altering *AMt2* levels significantly impacted *Wolbachia* titer in cells. Quantitative PCR was
257 thus used to measure relative *Wolbachia* titer in cells transfected with FLAG-AMt2 or FLAG-
258 empty. However, no changes in endosymbiont titer were observed following ectopic *AMt2*
259 expression; Unpaired two-tailed t-test with Welch's correction, $p = 0.1316$, $t = 1.794$, $df = 5.097$
260 (Fig 3C).

261 Reduced per-particle infectivity of viruses produced in the presence of *Wolbachia* (W+ viruses) is
262 associated with reduced replication kinetics of these viruses in vertebrate cells and reduced
263 infectivity of the encapsidated W+ virion RNA (11). As *AMt2* overexpression in *Wolbachia*-
264 colonized mosquito cells rescued viral RNA synthesis and progeny virus infectivity, we examined
265 the ability of progeny viruses derived from *Wolbachia*-colonized cells overexpressing *AMt2* (W+
266 AMt2+ cells) to replicate in vertebrate cells. We used a luciferase reporter based viral replication
267 assay following synchronous infection of three progeny virus types: W- virus, W+ virus and W+
268 AMt2+ virus over a period of 9 hours. Replication of W+ AMt2+ viruses were significantly higher
269 on a per-particle basis relative to both W+ and interestingly, W- viruses. This could be due higher
270 ectopic *AMt2* expression relative to what is induced natively during virus infection, implying
271 perhaps a dose-dependent effect; Tukey's multiple-comparisons test, Time: $p < 0.0001$,
272 *Wolbachia/AMt2*: $p = 0.0003$, Time X *Wolbachia/AMt2*: $p < 0.0001$ (Fig 3D). We then examined
273 whether ectopic *AMt2* expression caused changes in the infectivity of the virion encapsidated
274 RNA. Based on results from Fig 3C, we hypothesized that ectopic *AMt2* expression in *Wolbachia*-
275 colonized cells should restore virion RNA infectivity. Indeed, following transfection of virion RNA
276 into vertebrate BHK-21 cells, W+ virus-derived RNA was largely non-infectious in contrast to RNA
277 derived from W- and W+ AMt2+ viruses produced on average, two to three-fold more plaques
278 (Fig 3E). Restored infectivity of W+ AMt2+ virus derived RNA was also validated using the
279 luciferase-based virus replication assay, which mirrored the pattern observed previously with the
280 intact progeny virus particles in Fig 3D; One-way ANOVA followed by Tukey's post hoc test for
281 multivariate comparisons, w/ Wolb vs w/ Wolb + AMt2: $p < 0.00001$, w/o Wolb vs w/ Wolb: $p <$
282 0.0001; w/o Wolb vs w/ Wolb + AMt2: $p = 0.991$ (Fig 3F).

283 As demonstrated in Fig 2B, DNMT2 possesses the ability to bind viral RNA in mosquito cells.
284 However, this alone does not indicate whether its MTase activity is essential for its proviral role.
285 Broadly, DNMT2 is comprised of a catalytic domain, and a target recognition domain which is
286 responsible for RNA binding (19, 20). It is, therefore, possible that DNMT2's regulatory role is
287 independent of its MTase activity. To determine the importance of catalytic activity, we
288 overexpressed a catalytically-inactive mutant of *AMt2*, replacing the highly conserved cysteine
289 residue (C78) present in the motif IV region with a glycine (*AMt2* C78G, Fig 4A), in *Wolbachia*-
290 colonized mosquito cells and asked whether this allele is capable of relieving pathogen blocking.
291 Our data show *AMt2*-mediated rescue of SINV RNA synthesis and infectivity depends on its
292 MTase activity as expression of the C78G mutant failed to rescue virus from *Wolbachia*-mediated
293 inhibition; SINV: Unpaired t-test with Welch's correction, $p = 0.1734$, $t = 1.920$, $df = 2.396$ (Fig
294 4B). We observed no improvement in SINV infectivity under these conditions; Unpaired t-test with
295 Welch's correction, $p = 0.4544$, $t = 0.8291$, $df = 3.937$ (Fig 4C). Similar results were obtained from
296 experiments carried out using CHIKV, where expression of wild-type *AMt2*, but not *AMt2-C78G,*
297 resulted in improved virus titer; One-way ANOVA followed by Tukey's post hoc test for multivariate
298 comparisons, w/ Wolb vs w/ Wolb + AMt2, $p = 0.0009$, w/ Wolb vs w/ Wolb + AMt2 C78G $p =$
299 0.2694, w/ Wolb + AMt2 vs w/ Wolb + AMt2 C78G $p < 0.0040$ (Fig 4D,E). Based on these results,
300 we conclude that the MTase *AMt2* promotes virus infection in mosquitoes, and that lower *AMt2*

301 expression in the presence of *Wolbachia* contributes to virus restriction, and the MTase activity
302 of the *AMt2*-encoded DNMT2 is required for proviral function.

303 **DNMT2 orthologs from mosquitoes and fruit flies regulate virus infection differentially in**
304 **their respective hosts**

305 The proviral role of the *AMt2* is intriguing, given the previously described antiviral role for the
306 corresponding fruit fly DNMT2 ortholog, *Mt2* (9, 13). Interestingly, in our previous study, we
307 observed that knocking down *Mt2* led to an increase in progeny virus infectivity. Therefore, we
308 reasoned that ectopic expression of *Mt2* should reduce Sindbis virus infectivity (Fig S4). As with
309 mosquito *AMt2,* we asked whether this involved direct targeting of viral RNA. Direct interactions
310 between viral RNA and fly DNMT2 was confirmed by AZA-IP of epitope-tagged *Mt2* in *Wolbachia*-
311 free *Drosophila melanogaster*-derived JW18 cells, which showed a 10-fold enrichment in SINV
312 RNA-binding relative to a control host transcript (18S); One-sample two-tailed t-test performed on
313 log-transformed values, $p = 0.001$, $t = 4.462$, $df = 11$ (Fig S4A,B).

314 Regarding its effect on virus fitness, in contrast to the proviral effect of mosquito *AMt2*, ectopic
315 *Mt2* expression significantly reduced infectivity of progeny SINV and CHIKV (W- Mt2+ virus)
316 relative to those produced from cells expressing the control vector (W- virus), confirming our
317 previous findings; Unpaired two-tailed t-test with Welch's correction, SINV, $p = 0.0045$, $t = 3.698$,
318 $df = 9.458$, CHIKV, $p < 0.0001$, $t = 9.608$, $df = 6.926$ (Fig S4C). As with *AMt2,* we assessed
319 whether reduced infectivity of W- Mt2+ viruses was due to their inability to replicate in vertebrate
320 cells. Indeed, results from our luciferase reporter based viral replication assay revealed
321 significantly reduced replication of W- Mt2+ viruses relative to W- viruses in vertebrate BHK-21
322 cells, but similar to the behavior observed for W+ viruses; Two-way ANOVA Tukey's multiple
323 comparisons test, Time: $p < 0.0001$, *Wolbachia/AMt2*: $p = 0.0002$, Time X *Wolbachia/AMt2*: $p <$
324 0.0001 (Fig S4D). Finally, we quantified the infectivity of virion encapsidated RNA derived from
325 W- Mt2+ SINV and CHIKV viruses by measuring the number of plaque-forming units generated
326 following transfection into vertebrate BHK-21 cells. For both SINV and CHIKV, infectivity of virion
327 encapsidated RNA was reduced for W+ viruses. Notably, this was phenocopied by virion RNA
328 isolated from W- Mt2+ SINV and CHIKV; One-way ANOVA with Tukey's post hoc test for
329 multivariate comparisons: SINV, W- virus vs W+ virus, $p = 0.0409$, W- virus vs W- Mt2+ virus, p
330 $= 0.0052$, W+ virus vs W- Mt2+ virus, $p = 0.5122$, CHIKV, W- virus vs W+ virus, $p = 0.0005$, W-
331 virus vs W- Mt2+ virus, $p = 0.0045$, W+ virus vs W- Mt2+ virus, $p = 0.1571$ (Fig S4E,F).

332 Akin to mosquito *AMt2,* fly *Mt2's* ability to regulate virus fitness also rely on its catalytic activity,
333 as expressing a catalytically inactive mutant (*Mt2* C78A) was unable to restrict the production of
334 infectious virus and per-particle infectivity of SINV; One-way ANOVA with Tukey's post hoc test
335 for multivariate comparisons: Virus titer, w/o wMel vs w/o *w*Mel + Mt2, $p = 0.0011$, w/o wMel vs
336 w/o *w*Mel + Mt2 C78A, $p = 0.1034$, w/o wMel + Mt2 vs w/o *w*Mel + Mt2 C78A, $p = 0.0310$, Specific
337 Infectivity, w/o wMel vs w/o *w*Mel + Mt2, $p = 0.0047$, w/o wMel vs w/o *w*Mel + Mt2 C78A, $p =$
338 0.6269, w/o wMel + Mt2 vs w/o *w*Mel + Mt2 C78A, $p = 0.0194$ (Fig S5).

339 Taken together, these results suggest that progeny virus/virion RNA infectivity is reduced in fly
340 cells under conditions where MTase expression is elevated natively in the presence of *Wolbachia*
341 (W+ virus) or artificially (W- Mt2+ virus).

342 **Presence of *Wolbachia* in mosquito cells is associated with altered viral RNA methylation**

343 The fact that ectopic *AMt2* expression in *Wolbachia*-colonized *Aedes albopictus* cells is able to
344 restore the infectivity of SINV progeny virion RNA suggests two important things: 1. That the

Sindbis virion RNA carry 5-methylcytosine (m5C) modifications, and 2. That altered *AMt2* expression in the presence of *Wolbachia* is associated with changes in the overall m5C content of the virion RNA, which is likely restored upon ectopic MTase expression in *Aedes* cells. To directly determine if virus RNA is modified differentially in the presence of *Wolbachia*, we subjected virion RNA isolated from progeny SINV produced from *Aedes albopictus* cells colonized with (W+ virus) and without (W- virus) *Wolbachia* to liquid chromatography, followed by mass spectrometry (LC-MS/MS) analyses (Figure 5A). For our present analyses, we chose to focus our efforts on identifying the presence of 5-methylcytosine (m5C) as well as 6-methyladenosine (m6A) residues on the viral genome. We examined m6A due to recent reports that highlight the importance of this modification in regulating RNA virus replication (5, 21). A potential complication for these analyses is the presence of residue(s) of similar mass to charge ratio(s) to m5C such as m3C. However, as shown in Fig S6A, we were able to observe distinct distribution of the individual m3C and m5C peaks in the spectral output demonstrating our ability to distinguish between these two bases (Fig S6A).

LC-MS/MS analyses of RNA purified from virion RNA derived from *Wolbachia* free (W-), and *Wolbachia*-colonized (W+) cells demonstrated W+ virion RNA to contain on average, more than 2-fold less m5C residues compared to W- virion RNA across three independent virus preps from each cell type: Unpaired two-tailed t-test, $p = 0.0013$, $t = 8.080$, $df = 4$ (Figure 5B). Notably, both W+ and W- virion RNA was determined to consist of comparable levels of m6A residues across all biological replicates; Unpaired two-tailed t-test, $p = 0.666$, $t = 0.4643$, $df = 4$ (Figure 5C). In addition, we observed no significant changes in the overall m3C content between W+ and W- virion RNA; Unpaired two-tailed t-test, $p = 0.8068$, $t = 0.2612$, $df = 4$ (Fig S6B). It should be noted that while we did not observe changes in the overall abundance of m6A and m3C residues between W+ and W- virion RNA, it is unclear whether the presence of *Wolbachia* leads to altered distribution of m6A and/or m3C modifications in the context of the overall SINV RNA sequence. Finally, we used LC-MS/MS analyses to quantify viral Type-0 (7-methyl-GpppNp or M7G) cap structures present in W- and W+ virion RNA in order to estimate relative ratios of capped versus non-capped virus progeny produced in the presence or absence of *Wolbachia*. While there were no statistically significant differences present between the respective W- and W+ sample means, we found M7G content to vary significantly among W+ virion RNA replicates, indicating that the ratios of capped vs non-capped viruses vary significantly within virus populations derived from *Wolbachia*-colonized cells; Unpaired two-tailed t-test with Welch's correction and F-test to compare variances: $p > 0.999$, $t = 0.0014$, $df = 2.018$, $F = 227.4$, $DFn = 2$, $Dfd = 2$, $p = 0.0088$ (Fig S6C).

These data are consistent with: (i) DNMT2 being a required host factor in mosquito cells for efficient virus replication and transmission, (ii) this proviral effect being exert through m5C modification of the viral genomic RNA, and (iii) a mechanism of *Wolbachia*-mediated pathogen blocking being the reduction of DNMT2 expression.

Discussion

Virus inhibition in *Wolbachia*-colonized arthropods is associated with two distinct features that are independent of any particular host-*Wolbachia* strain combination; 1. reduced genome replication of the +ssRNA viruses in *Wolbachia*-colonized cells and 2. reduced per-particle infectivity of progeny +ssRNA viruses produced under these conditions (11). While these shared attributes constitute a subset of several virus inhibition phenotypes, it indicates the existence of a conserved

394 cellular mechanism of restriction. In our previous study, we used the prototype alphavirus, Sindbis
395 as our +ssRNA virus model to uncover an important role of the fruit fly RNA cytosine
396 methyltransferase (MTase) gene *Mt2* (DNMT2) as a required host determinant of *Wolbachia*-
397 mediated pathogen blocking (9). Notably, loss of *Drosophila* DNMT2 is associated with a loss in
398 virus inhibition by *Wolbachia*, which suggests that DNMT2 might regulate these two aspects of
399 alphavirus replication. These findings thus led us to ask the following question in our present
400 study: Is DNMT2 a conserved host determinant of *Wolbachia*-mediated +ssRNA virus inhibition
401 between fruit flies and mosquitoes? This work demonstrates the importance of *Aedes* DNMT2 in
402 pathogen blocking and introduces a wider, *Wolbachia*-independent role of this cytosine MTase in
403 alphavirus regulation across two dipteran genera.
404
405 MTase expression in adult *Aedes aegypti* mosquitoes is distinctly altered in the presence of both
406 virus and *Wolbachia,* and in opposite directions (Fig 1). DNMT2 expression is elevated following
407 an infectious bloodmeal, notably in the salivary gland tissues, which represent the final site of
408 virus production in the vector prior to transmission into a vertebrate. We show that this is likely to
409 the benefit of the virus, as ectopic MTase expression in cultured, *Wolbachia*-free *Aedes albopictus*
410 mosquito cells promote virus replication and importantly, progeny virus infectivity. Notably, this
411 phenomenon also occurs during DENV-2 infection in *w*Mel-colonized *Aedes aegypti* mosquitoes
412 (16). Indeed, baseline MTase activity is required for virus replication and spread in *Aedes* cells
413 (Fig S3). Furthermore, the extent to which virus replication is affected by the MTase inhibitor
414 depend on the virus source, and viruses produced from *Wolbachia*-colonized cells (W+ viruses)
415 are more susceptible to MTase inhibition. It should be noted that this outcome phenocopies the
416 scenario wherein virus spread is most restricted under conditions where both producer and target
417 mosquito cells are colonized with *Wolbachia* (11). In line with these findings, our data indicate
418 loss in MTase expression occurring in the presence of *Wolbachia* (Fig 1). This observation is also
419 in line with previous reports (16). With regards to the mechanism of DNMT2's role in pathogen
420 blocking in mosquitoes, our collective data support a model in which endosymbiont-induced
421 reduction in MTase expression and catalytic MTase function contribute to losses in virus
422 replication and per-particle infectivity (Fig 3-4). This consequently limits virus dissemination within
423 the mosquito vector, as well as transmission to a vertebrate host (Fig 3-4). Given that our results
424 are analogous to prior reports involving a different RNA virus and *Wolbachia* strain suggests that
425 the interaction between virus, *Wolbachia* and host MTase expression is likely independent of any
426 particular virus-host-*Wolbachia* combination, representing a conserved feature of pathogen
427 blocking in the native *Aedes* vector.
428
429 At the molecular level, our data demonstrate interaction between DNMT2 orthologs from *Aedes*
430 *albopictus* and *Drosophila melanogaster* and viral RNA (Fig 4B, Fig S5B) (11). It remains to be
431 seen whether these interactions are analogous to DNMT2-DCV RNA interactions in *Drosophila,*
432 where the MTase-viral RNA binding occurs specifically at structured viral Internal Ribosomal Entry
433 Sites (IRES) (13). Additionally, it is unclear if DNMT2 interactions in the mosquito cell is specific
434 for viral RNA or whether it extends to host transcripts. Future studies involving PARCLIP-
435 sequencing of immunoprecipitated DNMT2-RNA complexes should allow identification and
436 mapping of distinct DNMT2-binding motifs and/or structural elements within viral and host RNA
437 species. Nevertheless,
438 how is DNMT2 recruited to the viral RNA and which viral and host proteins are required for
439 recruitment? Assuming that the proviral role of DNMT2 involves addition of m5C signatures to
440 specific residues on the viral genome, it is likely that it requires co-operative interactions between
441 DNMT2 and viral co-factor(s). However, that DNMT2 is antiviral in fruit flies raises the possibility

442 of this interaction involving *Aedes*-specific host factors that are absent in *Drosophila melanogaster*
443 (22).
444
445 Consistent with DNMT2's role as a cytosine MTase, m5C content of virion RNA produced from
446 *Wolbachia*-colonized cells (W+ viruses) is significantly reduced relative to cells without the
447 symbiont (Fig 5B) (11). Incidentally, this finding follow reports dating back several decades
448 describing the occurrence of m5C residues within intracellular SINV RNA (23). The initial
449 hypotheses proposing the involvement of these intracellular m5C signatures in alphavirus
450 genome replication is supported by our observation that W+ virion RNA, which are presumably
451 hypomethylated, are less infectious on a per-genome basis (Fig 3E-F) (24). Indeed, based on our
452 data, we can infer that these m5C modifications regulate alphavirus infection across multiple hosts
453 and thus by extension, aspects of the virus transmission cycle. It should also be noted that while
454 methylated nucleotide residues like m6A and m5C occur on RNA virus genomes at rates that are
455 an order of magnitude higher than those present in cellular RNA species, our results do not
456 exclude the possibility of other RNA modifications, as well as differential modification of host RNA
457 species and their potential role in pathogen blocking, especially given recent evidence of altered
458 m6A modification of specific cellular transcripts during flavivirus infection in vertebrate cells (21,
459 25, 26).
460
461 How these modifications influence virus replication in a cell is still an open question. Indeed,
462 information regarding the functional consequence of m5C or other RNA modifications on viral
463 RNA is limited, and while we may be able to draw certain conclusions based on our current
464 knowledge of known eukaryotic RNA modifications, the potential implications of arbovirus RNA
465 methylation may be broader than we are currently able to anticipate (27). We can hypothesize
466 that differential viral methylation may alter host responses to infection, in that depending on the
467 host or cell type, as well as the genomic context of methylation, the presence or absence of m5C
468 may either allow detection by and/or provide a mechanism of escape from RNA-binding proteins
469 (e.g., Dicer, RIG-I, MDA5, TLRs, APOBEC3) involved in virus restriction or non-self RNA
470 recognition that trigger downstream immune signaling and interferon production (28). Differential
471 modifications of viral RNA may thus also regulate different cytological outcomes of arboviruses in
472 arthropod cells i.e., persistence versus mammalian cells i.e., cell death. It remains to be seen
473 whether or not one or more these situations occur during pathogen blocking, and if W- and W+
474 viruses trigger differential innate immune responses in vertebrate cells.
475
476 Based on our data, we propose a model in which our current estimates of m5C residues on W-
477 viruses represent the "wild-type" epitranscriptome of mosquito-derived alphavirus. In naïve
478 vertebrate cells, presence of these signatures allows viruses to replicate efficiently following
479 successful evasion of host innate immunity. In contrast, m5C hypomethylation of W+ viruses
480 render them more susceptible to host induced restriction, thus impacting their ability to propagate.
481 Aside from heightened immune susceptibility, fitness of hypomethylated W+ viruses could also
482 result from reduced incoming viral RNA stability and/or translation. Given that pharmacological
483 inhibition of MTase activity impact virus spread in mosquito cells, it is likely that W+ virus
484 hypomethylation also influence dissemination in arthropod cells (11). It is also possible that other
485 factors contribute to the reduced fitness of W+ viruses. In particular, our LC-MS/MS analyses
486 suggest increased heterogeneity in m7G moiety abundance on W+ virion RNA, indicating a
487 potential imbalance in viral RNA capping in the presence of *Wolbachia.* Past work has shown that
488 SINV populations derived from different hosts vary with regards to the ratios of capped and non-
489 capped SINV RNA (29). Despite being important for alphavirus replication, non-capped SINV
490 RNA alone are compromised in their ability to undergo translation, are more susceptible to RNA

491 decay machineries and have been shown to induce elevated innate immune response, all of
492 which might contribute to the observed loss in infectivity.
493
494 Finally, the data presented here implicating epitranscriptomic regulation of alphaviruses unlocks
495 multiple avenues of investigation, which include, but are not limited to the following. First, it is
496 important to determine the genomic context of m5C and other RNA modifications on viral RNA
497 with respect to different hosts, cell types and timeline of infection, which may be achieved by long-
498 read, direct sequencing of RNA from virus-infected cells. Doing so would not only allow sequence-
499 specific mapping of these signatures, but also help address the question whether virus infection
500 is regulated solely via targeting of viral RNA by cellular MTases. Furthermore, deriving mapping
501 information might inform us whether modifications are directed to specific RNA elements that
502 result in spatiotemporal changes in RNA structure and altered base-pairing, thus regulating virus
503 RNA polymerase fidelity and/or translation in the cell. Additional areas of inquiry involve identifying
504 cellular pathways responsible for determining the fate of W+ viruses as well as characterizing the
505 functional consequences of abolishing highly conserved m5C residues on the viral RNA. This
506 would allow further exploration into the effect of these signatures on RNA stability, gene
507 expression and/or packaging across arthropod and vertebrate cells. Lastly, unlike m6A-
508 modifications, little is known regarding how m5C signatures are interpreted i.e., how they are
509 "read", "maintained" and "erased", in mammalian and to an even lesser extent, in arthropod cells
510 (27). Promising candidates include m5C-binding "reader" proteins ALYREF and YBX1, which
511 function alongside the known cellular m5C MTase NSUN2 to influence mRNA nuclear transport
512 and stability (30, 31). Following approaches described in recent studies, identification of these
513 RNA-binding proteins, either viral or host-derived, may be achieved via affinity-based
514 immunoprecipitation of viral RNA and form the basis of future studies (32).
515
516 Alphaviruses, like most other RNA viruses, are limited in their coding capacity and are known to
517 alter their genome structure under various cellular conditions to regulate aspects of its own
518 replication as a way to maximize viral genome functionality. Echoing this idea, the findings
519 presented in this study add an additional regulatory mechanism adopted by these viruses to
520 successfully navigate within and transition between vertebrate and arthropod host species.
521
522
523 **Materials and Methods**
524
525 **Insect and Mammalian Cell Culture**
526 RML12 *Aedes albopictus* cells with and *Wolbachia*-free *w*Mel were grown at 24 ºC in Schneider's
527 insect media (Sigma-Aldrich) supplemented with 10% heat-inactivated fetal bovine serum
528 (Corning), 1% each of L-Glutamine (Corning), non-essential amino acids (Corning) and penicillin-
529 streptomycin-antimycotic (Corning). C7-10 *Aedes albopictus* cells with and *Wolbachia*-free were
530 grown at 27 ºC under 5% ambient CO_2 in 1X Minimal Essential Medium (Corning) supplemented
531 with 5% heat-inactivated fetal bovine serum (Corning), 1% each of L-Glutamine (Corning), non-
532 essential amino acids (Corning) and penicillin-streptomycin-antimycotic (Corning). Vertebrate
533 baby hamster kidney fibroblast or BHK-21 cells were grown at 37 ºC under 5% ambient CO_2 in
534 1X Minimal Essential Medium (Corning) supplemented with 10% heat-inactivated fetal bovine
535 serum (Corning), 1% each of L-Glutamine (Corning), non-essential amino acids (Corning) and
536 penicillin-streptomycin-antimycotic (Corning).

537 **Mosquito rearing and blood meals**

538 *Aedes aegypti* mosquitoes either -infected and -uninfected with *Wolbachia* (wAlbB strain)
539 (generously provided by Dr. Zhiyong Xi, Michigan State University, USA), were reared in an insect
540 incubator (Percival Model I-36VL, Perry, IA, USA) at 28 °C and 75% humidity with 12 h light/dark
541 cycle. Four to six-day old mated female mosquitoes were allowed to feed for 1h on approximately
542 10^8 PFUs of SINV (TE12-untagged) containing citrated rabbit blood (Fisher Scientific DRB030)
543 supplemented with 1mM ATP (VWR) and 10% sucrose using a Hemotek artificial blood feeding
544 system (Hemotek, UK) maintained under constant temperature of 37 °C. Engorged mosquitoes
545 were then isolated and reared at 28 °C in the presence of male mosquitoes. For harvesting whole
546 tissues, mosquitoes were harvested 5-7 days post blood meal before being snap frozen in liquid
547 nitrogen and stored at −80 °C before further processing. For salivary gland dissections,
548 mosquitoes were kept immobilized on ice prior to dissection. Collected salivary gland tissues were
549 washed three-times in cold, sterile saline solution (1XPBS) prior to being snap frozen in liquid
550 nitrogen and stored at −80 °C before further processing. Three-salivary glands were pooled to
551 create each biological replicate. Samples for qPCR and qRT-PCR were homogenized in TRiZOL
552 (Sigma Aldrich) reagent and further processed for nucleic acid extractions using manufacturer's
553 protocols.

554 **Virion RNA extraction and transfection into cells**

555 Virion encapsidated RNA was extracted from viruses (SINV-nLuc) purified over a 27% sucrose
556 cushion using TRiZOL reagent (Sigma Aldrich) using manufacturer's protocol. Post extraction,
557 RNAs were DNase (RQ1 RNase-free DNase, NEB) treated using manufacturer's protocol to
558 remove cellular contaminants and viral RNA copies were quantified using quantitative RT-PCR
559 using primers probing for SINV nsP1 and E1 genomic regions (Primer Table). To determine
560 infectivity or replication kinetics of virion derived RNA, equal copies of viral RNA or equal mass of
561 virion derived total RNA, quantified using qRT-PCR, were transfected into BHK-21 cells for SINV
562 in serum-free Opti-MEM (Gibco). Transfection was carried out for 6 hours before the transfection
563 inoculum was removed, and overlay was applied. Cells were fixed 48 hours post transfection for
564 SINV using 10% (v/v) formaldehyde and stained with crystal violet to visualize plaques.

565 **Viral replication assays**

566 Quantification of viral genome and sub-genome translation was performed using cellular lysates
567 following synchronized infections with reporter viruses (SINV-nLuc), or transfections with virion-
568 derived RNA from the aforementioned viruses. At indicated times post infection, samples were
569 collected and homogenized in 1X Cell Culture Lysis Reagent (Promega). Samples were mixed
570 with NanoGlo luciferase reagent (Promega), incubated at room temperature for 3 minutes before
571 luminescence was recorded using a Synergy H1 microplate reader (BioTech instruments).

572 **DNMT2 overexpression in *Aedes* cells**

573 *Aedes albopictus AMt2* coding region was subcloned into PCR 2.1 TOPO vector (Invitrogen) by
574 PCR amplification of cDNA generated using reverse transcribed from total cellular RNA isolated
575 from C636 *Aedes albopictus* cells using Protoscript II RT (NEB) and oligo-dT primers (IDT).
576 Coding region was validated via sequencing before cloned into the pAFW expression vector
577 (1111) (Gateway Vector Resources, DGRC), downstream of and in-frame with the 3X FLAG tag
578 using the native restriction sites AgeI and NheI (NEB). Expression of both FLAG-tagged
579 AaDNMT2 in mosquito cells was confirmed using qRT-PCR and Western Blots using an anti-
580 FLAG monoclonal antibody (SAB4301135 - Sigma-Aldrich) (Fig 4A). Catalytic MTase mutant of
581 *AMt2* (*AMt2*-C78G*),* was generated via site-directed mutagenesis (NEB, Q5 Site-Directed
582 Mutagenesis Kit). using primers listed in the primer table (Table S1).

583 **Immunoprecipitation of DNMT2-viral RNA complexes**

584 JW18 fly cells and C7-10 mosquito cells were transfected with expression vectors FLAG-Mt2 and
585 FLAG-AMt2 respectively for 48 hours prior to infection with SINV at MOI of 10. Control cells were
586 transfected with the empty vector plasmid FLAG-empty. Cells were treated for approximately 18h
587 with 5 μM 5-Azacytidine to covalently trap Mt2 or AMt2 with its target cellular RNA prior to RNA
588 immunoprecipitation using anti-FLAG antibody (17).

589 **Real-time quantitative RT-PCR analyses**

590 Following total RNA extraction using TRiZOL reagent, cDNA was synthesized using MMuLV
591 Reverse Transcriptase (NEB) with random hexamer primers (Integrated DNA Technologies).
592 Negative (no RT) controls were performed for each target. Quantitative RT-PCR analyses were
593 performed using Brilliant III SYBR green QPCR master mix (Bioline) with gene-specific primers
594 according to the manufacturer's protocol and with the Applied Bioscience StepOnePlus qRT-PCR
595 machine (Life Technologies). The expression levels were normalized to the endogenous 18S
596 rRNA expression using the delta-delta comparative threshold method (ΔΔCT). Fold changes were
597 determined using the comparative threshold cycle (CT) method (Table S1). Efficiencies for primer
598 sets used in this study have been validated in our previous study (11).

599 **Virion RNA extraction and transfection**

600 Virion encapsidated RNA was extracted from viruses (SINV-nLuc) were purified over a 27%
601 sucrose cushion using TRiZOL reagent (Sigma Aldrich) using manufacturer's protocol. Post
602 extraction, RNAs were DNase (RQ1 RNase-free DNase, NEB) treated using manufacturer's
603 protocol to remove cellular contaminants and viral RNA copies were quantified via quantitative
604 RT-PCR using primers probing for SINV nsP1 and E1 genomic regions (Table S1) and a standard
605 curve comprised of linearized SINV infectious clone containing the full-length viral genome. To
606 determine infectivity or replication kinetics of Sindbis virion RNA, equal copies of virion isolated
607 RNA (10^5 copies), quantified using qRT-PCR, were transfected into BHK-21 cells in serum-free
608 Opti-MEM (Gibco). Transfection was carried out for 6 hours before the transfection inoculum was
609 removed, and overlay was applied. Cells were fixed 48 hours post transfection using 10% (v/v)
610 formaldehyde and stained with crystal violet to visualize plaques.

611 **Quantification of RNA modifications by LC-MS/MS**

612 Total RNA (3-7μg) was digested by nuclease P1 (10 Units) at 50°C for 16 hr. Additional Tris pH
613 7.5 was then added to a final concentration of 100 mM to adjust the pH, which was followed by
614 the addition of calf intestinal alkaline phosphatase (CIP, NEB, 2Units). The mixture was incubated
615 at 37°C for 1 hour to convert nucleotide 5'-monophosophates to their respective nucleosides. 10μl
616 of RNA samples were diluted to 30 μL and filtered (0.22 μm pore size). 10μL of the sample was
617 used for LC-MS/MS. Briefly, nucleosides were separated on a C18 column (Zorbax Eclipse Plus
618 C18 column, 2.1 x 50mm, 1.8 Micron) paired with an Agilent 6490 QQQ triple-quadrupole LC
619 mass spectrometer using multiple-reaction monitoring in positive-ion mode. The nucleosides were
620 quantified using the retention time of the pure standards and the nucleoside to base ion mass
621 transitions of 268.1 to 136 (A), 244.1 to 112 (C), 284.2 to 152 (G), 300 to 168.1 (8-oxoG), 282.2
622 to 150 (m1A), 298 to 166 (m1G), 258 to 126 (m3C and m5C), 282.1 to 150 (m6A), 298 to 166
623 (m7G). Standard-calibration curves were generated for each nucleoside by fitting the signal
624 intensities against concentrations of pure-nucleoside preparations. The curves were used to
625 determine the concentration of the respective nucleoside in the sample. The A, G, and C
626 standards were purchased from ACROS ORGANICS; m5C was purchased from BioVision; m7G,
627 m1G and m3C were purchased from Carbosynth, m6G and m6A were purchased from Berry's

Associates, and m1A was from Cayman Chemical Company. The modification level on the nucleosides was calculated as the ratio of modified: unmodified.

Statistical analyses of experimental data

All statistical analyses were conducted using GraphPad Prism 8 (GraphPad Software Inc., San Diego, CA).

Graphics

Graphical assets made in © BioRender - biorender.com.

Acknowledgments

We thank members of the Hardy, Newton, Danthi, Mukhopadhyay and Patton Labs for critical proof-reading of the manuscript and for fostering ideas through helpful discussions. We thank the staff at the Center for Genomics and Bioinformatics (CGB), Indiana University Bloomington, for their help with performing nanopore sequencing workflow. We thank Dr. David Mackenzie-Liu for generating the original cloning vector with the SacI restriction site. We thank our colleagues outside of IU for their generosity in sharing reagents, including Dr. Horacio Frydman, Boston University for providing us Aa23 and C7-10 *Aedes albopictus* cells, Dr. William Sullivan for providing us with JW18 *Drosophila melanogaster* cells, and Dr. Zhiyong Xi, Michigan State University for providing us *Aedes aegypti* mosquitoes. This work was supported by NSF award to ILGN and RWH (MTM2025389), NIH R01 to ILGN (R01AI144430), NIH R21 to RWH (R21AI153785).

References

1. D. Mackenzie-Liu, K. J. Sokoloski, S. Purdy, R. W. Hardy, Encapsidated Host Factors in Alphavirus Particles Influence Midgut Infection of Aedes aegypti. *Viruses* **10** (2018).
2. K. J. Sokoloski *et al.*, Encapsidation of host-derived factors correlates with enhanced infectivity of Sindbis virus. *J Virol* **87**, 12216-12226 (2013).
3. C. A. Dunbar *et al.*, Dissecting the Components of Sindbis Virus from Arthropod and Vertebrate Hosts: Implications for Infectivity Differences. *ACS Infect Dis* **5**, 892-902 (2019).
4. P. Hsieh, M. R. Rosner, P. W. Robbins, Host-dependent variation of asparagine-linked oligosaccharides at individual glycosylation sites of Sindbis virus glycoproteins. *J Biol Chem* **258**, 2548-2554 (1983).
5. N. S. Gokhale *et al.*, N6-Methyladenosine in Flaviviridae Viral RNA Genomes Regulates Infection. *Cell Host Microbe* **20**, 654-665 (2016).
6. D. G. Courtney *et al.*, Epitranscriptomic Addition of m(5)C to HIV-1 Transcripts Regulates Viral Gene Expression. *Cell Host Microbe* **26**, 217-227.e216 (2019).
7. A. R. I. Lindsey, T. Bhattacharya, R. W. Hardy, I. L. G. Newton, Wolbachia and virus alter the host transcriptome at the interface of nucleotide metabolism pathways. *bioRxiv* 10.1101/2020.06.18.160317, 2020.2006.2018.160317 (2020).
8. A. R. I. Lindsey, T. Bhattacharya, I. L. G. Newton, R. W. Hardy, Conflict in the Intracellular Lives of Endosymbionts and Viruses: A Mechanistic Look at Wolbachia-Mediated Pathogen-blocking. *Viruses* **10** (2018).
9. T. Bhattacharya, I. L. Newton, R. W. Hardy, Wolbachia elevates host methyltransferase expression to block an RNA virus early during infection. *PLoS pathogens* **13**, e1006427 (2017).

673 10. T. Bhattacharya, I. L. G. Newton, Mi Casa es Su Casa: how an intracellular symbiont
674 manipulates host biology. *Environ Microbiol* 10.1111/1462-2920.13964 (2017).
675 11. T. Bhattacharya, I. L. G. Newton, R. W. Hardy, Viral RNA is a target for Wolbachia-
676 mediated pathogen blocking. *PLoS Pathog* **16**, e1008513 (2020).
677 12. M. Schaefer *et al.*, RNA methylation by Dnmt2 protects transfer RNAs against stress-
678 induced cleavage. *Genes & development* **24**, 1590-1595 (2010).
679 13. Z. Durdevic *et al.*, Efficient RNA virus control in Drosophila requires the RNA
680 methyltransferase Dnmt2. *EMBO reports* **14**, 269-275 (2013).
681 14. S. Phalke *et al.*, Retrotransposon silencing and telomere integrity in somatic cells of
682 Drosophila depends on the cytosine-5 methyltransferase DNMT2. *Nat Genet* **41**, 696-
683 702 (2009).
684 15. Z. Durdevic, M. Schaefer, Dnmt2 methyltransferases and immunity: an ancient
685 overlooked connection between nucleotide modification and host defense? *Bioessays*
686 **35**, 1044-1049 (2013).
687 16. G. Zhang, M. Hussain, S. L. O'Neill, S. Asgari, Wolbachia uses a host microRNA to
688 regulate transcripts of a methyltransferase, contributing to dengue virus inhibition in
689 Aedes aegypti. *Proc Natl Acad Sci U S A* **110**, 10276-10281 (2013).
690 17. V. Khoddami, B. R. Cairns, Transcriptome-wide target profiling of RNA cytosine
691 methyltransferases using the mechanism-based enrichment procedure Aza-IP. *Nat*
692 *Protoc* **9**, 337-361 (2014).
693 18. M. G. Goll *et al.*, Methylation of tRNAAsp by the DNA methyltransferase homolog
694 Dnmt2. *Science* **311**, 395-398 (2006).
695 19. A. Jeltsch *et al.*, Mechanism and biological role of Dnmt2 in nucleic acid methylation.
696 *RNA biology* **14**, 1108-1123 (2017).
697 20. T. P. Jurkowski *et al.*, Human DNMT2 methylates tRNAAsp molecules using a DNA
698 methyltransferase-like catalytic mechanism. *Rna* **14**, 1663-1670 (2008).
699 21. W. McIntyre *et al.*, Positive-sense RNA viruses reveal the complexity and dynamics of
700 the cellular and viral epitranscriptomes during infection. *Nucleic Acids Res* **46**, 5776-
701 5791 (2018).
702 22. T. Bhattacharya, D. W. Rice, R. W. Hardy, I. Newton, Adaptive evolution in DNMT2
703 supports its role in the dipteran immune response. *bioRxiv* (2020).
704 23. D. T. Dubin, V. Stollar, Methylation of Sindbis virus "26S" messenger RNA. *Biochem*
705 *Biophys Res Commun* **66**, 1373-1379 (1975).
706 24. T. K. Frey, D. L. Gard, J. H. Strauss, Replication of Sindbis virus. VII. Location of 5-
707 methyl cytidine residues in virus-specific RNA. *Virology* **89**, 450-460 (1978).
708 25. N. S. Gokhale *et al.*, Altered m(6)A Modification of Specific Cellular Transcripts Affects
709 Flaviviridae Infection. *Mol Cell* **77**, 542-555.e548 (2020).
710 26. K. Tsai, B. R. Cullen, Epigenetic and epitranscriptomic regulation of viral replication. *Nat*
711 *Rev Microbiol* 10.1038/s41579-020-0382-3, 1-12 (2020).
712 27. R. Netzband, C. T. Pager, Epitranscriptomic marks: Emerging modulators of RNA virus
713 gene expression. *Wiley Interdiscip Rev RNA* **11**, e1576 (2020).
714 28. A. F. Durbin, C. Wang, J. Marcotrigiano, L. Gehrke, RNAs Containing Modified
715 Nucleotides Fail To Trigger RIG-I Conformational Changes for Innate Immune Signaling.
716 *mBio* **7** (2016).
717 29. K. Sokoloski, K. Haist, T. Morrison, S. Mukhopadhyay, R. Hardy, Noncapped alphavirus
718 genomic RNAs and their role during infection. *Journal of virology* **89**, 6080-6092 (2015).
719 30. X. Chen *et al.*, 5-methylcytosine promotes pathogenesis of bladder cancer through
720 stabilizing mRNAs. *Nat Cell Biol* **21**, 978-990 (2019).

721 31. X. Yang *et al.*, 5-methylcytosine promotes mRNA export - NSUN2 as the
722 methyltransferase and ALYREF as an m(5)C reader. *Cell Res* **27**, 606-625 (2017).
723 32. M. Garcia-Moreno, A. I. Järvelin, A. Castello, Unconventional RNA-binding proteins step
724 into the virus–host battlefront. *Wiley Interdisciplinary Reviews: RNA* **9**, e1498 (2018).

725

726

727 **Figures and Tables**

728

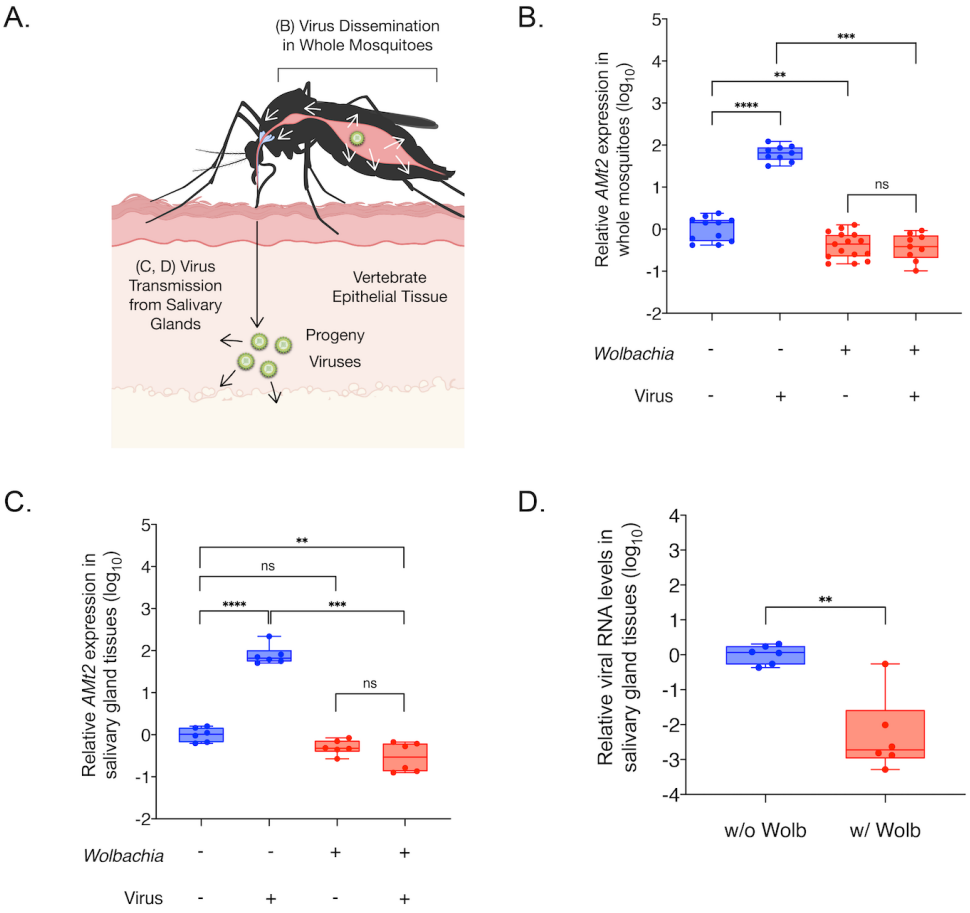

729
730 **Fig 1. Virus and *Wolbachia* each differentially modulate expression of the RNA methyltransferase**
731 **gene DNMT2 in mosquitoes.** (A) Schematic of virus dissemination (white arrows) within mosquito tissues
732 and transmission into vertebrate host (black arrow). (B) *AMt2* expression measured in 2-4-day old whole
733 female mosquitoes with and *Wolbachia*-free using qRT-PCR 5 days post bloodmeal with and without SINV.
734 Error bars represent standard error of mean (SEM) of biological replicates. Two-way ANOVA performed on
735 log-transformed data, followed by Tukey's multiple comparison test. Letters represent statistically significant
736 difference between mean values. (C) *AMt2* expression measured in dissected salivary gland tissues
737 collected from female mosquitoes with and *Wolbachia*-free 5 days post bloodmeal with or without SINV.
738 Error bars represent standard error of mean (SEM) of biological replicates. Two-way ANOVA performed on
739 log-transformed data, followed by Tukey's multiple comparison test. Letters represent statistically significant
740 difference between mean values. (D) Viral RNA levels were quantified in dissected salivary gland tissues
741 with and *Wolbachia*-free using qRT-PCR at 5 days post infectious blood meal with SINV. Error bars
742 represent standard error of mean (SEM) of biological replicates. Student's t-test performed on log-
743 transformed values. ****P < 0.0001.
744
745

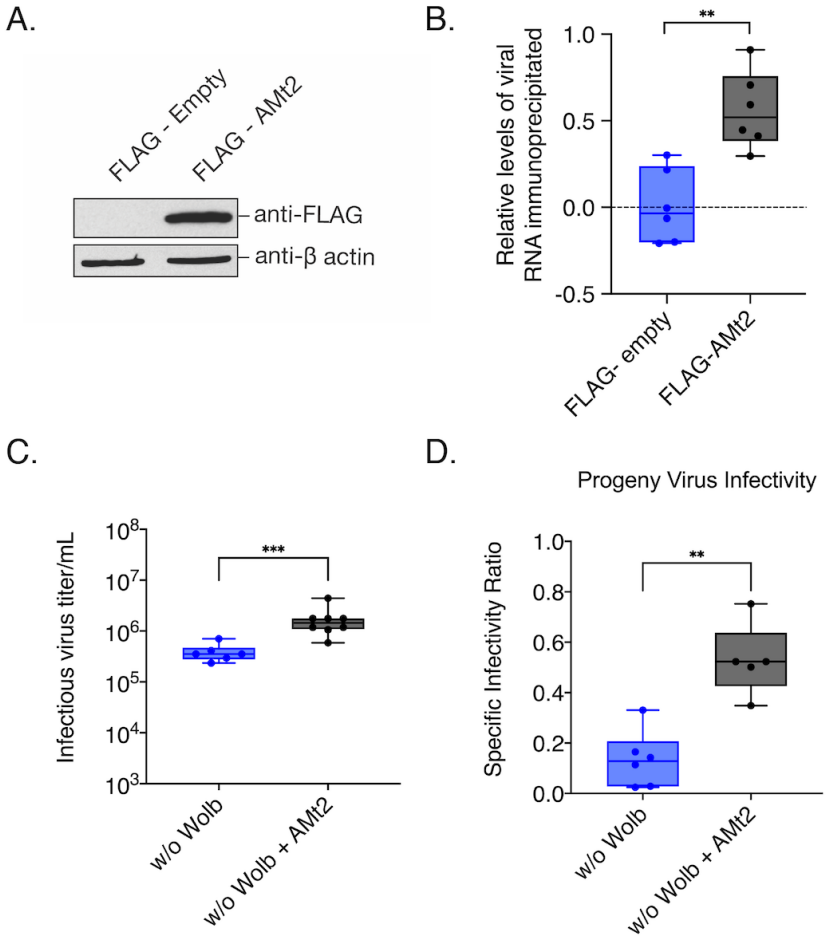

Fig 2. Overexpressing *AMt2* in mosquito cells improve progeny virus infectivity. (A) Western Blot of mosquito cells transfected with expression vector constructs with (FLAG-AMt2) or without (FLAG-empty) *AMt2.* Cytoplasmic lysates of cells were collected 48 hours post transfection and probed with anti-FLAG and anti-β actin antibodies. (B) Relative levels of viral RNA recovered following AZA-IP of AMt2 in mosquito cells was quantified using qRT-PCR. C7-10 mosquito cells *Wolbachia*-free were transfected with expression vectors FLAG-empty or FLAG-AMt2 for 48 hours prior to infection with SINV at MOI of 10. Cells were treated for approximately 18h with 5 μM 5-Azacytidine to covalently trap AMt2 with its target cellular RNA prior to RNA immunoprecipitation using anti-FLAG antibody. (C) Infectious progeny virus produced from mosquito cells *Wolbachia*-free expressing either FLAG-empty (w/o Wolb) or FLAG-AMt2 (w/o Wolb + AMt2). Mosquito cells were transfected 48 hours prior to infection with SINV at MOI of 10. Infectious progeny viruses collected from supernatants 48 hours post-infection were quantified using plaque assays on BHK-21 cells. (D) Specific Infectivity Ratios of progeny viruses were calculated as described earlier. Error bars represent standard error of mean (SEM) of biological replicates. **P < 0.01; ****P < 0.0001.

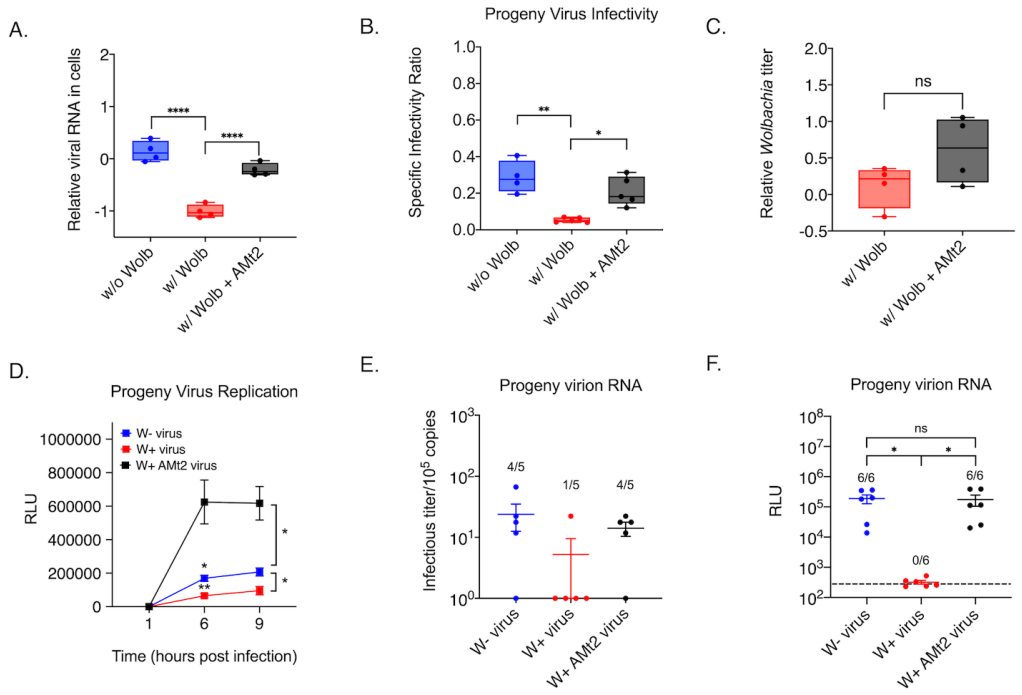

Fig 3. *AMt2* overexpression in *Wolbachia*-colonized mosquito cells rescues virus from endosymbiont-mediated inhibition. C7-10 mosquito cells with *Wolbachia* were transfected with expression vectors FLAG-empty (w/ Wolb) or FLAG-AMt2 (w/ Wolb + AMt2) for 48 hours prior to infection with SINV-nLuc at MOI of 10. *Wolbachia* -free cells expressing FLAG-empty (w/o Wolb) were used as a positive control. (A) Viral genome replication in mosquito cells was quantified using qRT-PCR using extracted total RNA from infected cell lysates. (B) Specific Infectivity Ratios of progeny viruses produced from Infectious progeny viruses collected from supernatants 48 hours post infection were quantified using plaque assays on BHK-21 cells, while total number of progeny virus particles was quantified via qRT-PCR of viral genome copies released into the supernatant. Error bars represent standard error of mean (SEM). (C) C7-10 mosquito cells with *Wolbachia* were transfected with expression vectors FLAG-empty (w/ Wolb) or FLAG-AMt2 (w/ Wolb + AMt2) for 48 hours prior to quantification of endosymbiont titer via quantitative PCR using DNA from extracted cell lysates. (D) Specific Infectivity Ratios of progeny viruses produced from the aforementioned infection was determined as described earlier. Error bars represent standard error of mean (SEM). Statistically non-significant values are indicated by ns. (E) Progeny viruses were used to synchronously infect naïve BHK-21 cells at equivalent MOIs of 5 particles/cell. Cell lysates were collected at indicated times post infection and luciferase activity (RLU), was used as a proxy for viral replication. (F) Approximately 10^5 copies each of virion encapsidated RNA extracted from the aforementioned W+, W+ AMt2 and W- viruses were transfected into naïve BHK-21 cells and infectious titer was determined by the counting the number of plaques produced after 72 hours post transfection. Numbers above bars refer to the proportion of samples that formed quantifiable plaque-forming units on BHK-21 cells. (G) 10^5 copies each of virion encapsidated RNA extracted from the W+, W+ AMt2 and W- viruses were transfected into naïve BHK-21 cells and luciferase activity (RLU) was used as a proxy for viral replication at 9 hours post-transfection. Numbers above bars refer to the proportion of samples that produced luciferase signal above background levels, indicated by the dotted line. Error bars represent standard error of mean (SEM). *P < 0.05; **P < 0.01; ****P < 0.0001.

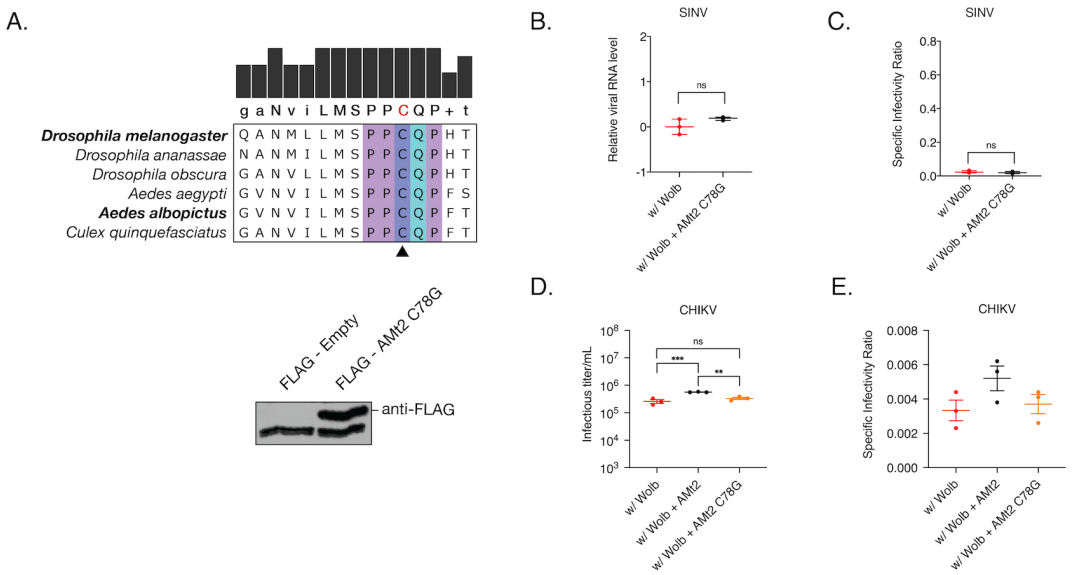

Fig 4: Catalytically inactive DNMT2 is unable to rescue *Wolbachia*-mediated virus inhibition in mosquito cells. (A) Multiple sequence alignment of the Motif IV region of DNMT2 derived from dipterans that are known to be colonized with native or non-native *Wolbachia.* The conserved catalytic cysteine (C) residue, depicted in red on the consensus sequence at the top, was mutated to a glycine (G) to abolish MTase activity of mosquito AMt2. Expression of the catalytic mutant (AMt2 C78G) was determined at 48 hours post transfection using Western Blot. C7-10 mosquito cells transfected with expression vector constructs with (FLAG-AMt2 C78G) or without (FLAG-empty) *AMt2.* Cytoplasmic lysates of cells were collected 48 hours post transfection and probed with anti-FLAG antibody. The non-specific band appearing below the desired size was used as a loading control. (B) C7-10 mosquito cells with *Wolbachia* were transfected with expression vectors FLAG-empty (w/ Wolb), FLAG-AMt2 (w/ Wolb + AMt2) or FLAG-C78G AMt2 (w/ Wolb + AMt2 C78G) for 48 hours prior to infection with CHIKV-mKate at MOI of 10. Infectious virus and Specific Infectivity (SI) of progeny viruses produced after 72 hours post infection were quantified as before. (C) C7-10 mosquito cells with *Wolbachia* were transfected with expression vectors FLAG-empty (w/ Wolb) or FLAG-AMt2 (w/ Wolb + AMt2). Effect of AMt2 overexpression on *Wolbachia* titer was determined by quantifying *wsp* genome copies via quantitative PCR of genomic DNA isolated from cells 48 hours post transfection. Error bars represent standard error of mean (SEM) of biological replicates. **P < 0.01; ***P < 0.001, ns = non-significant.

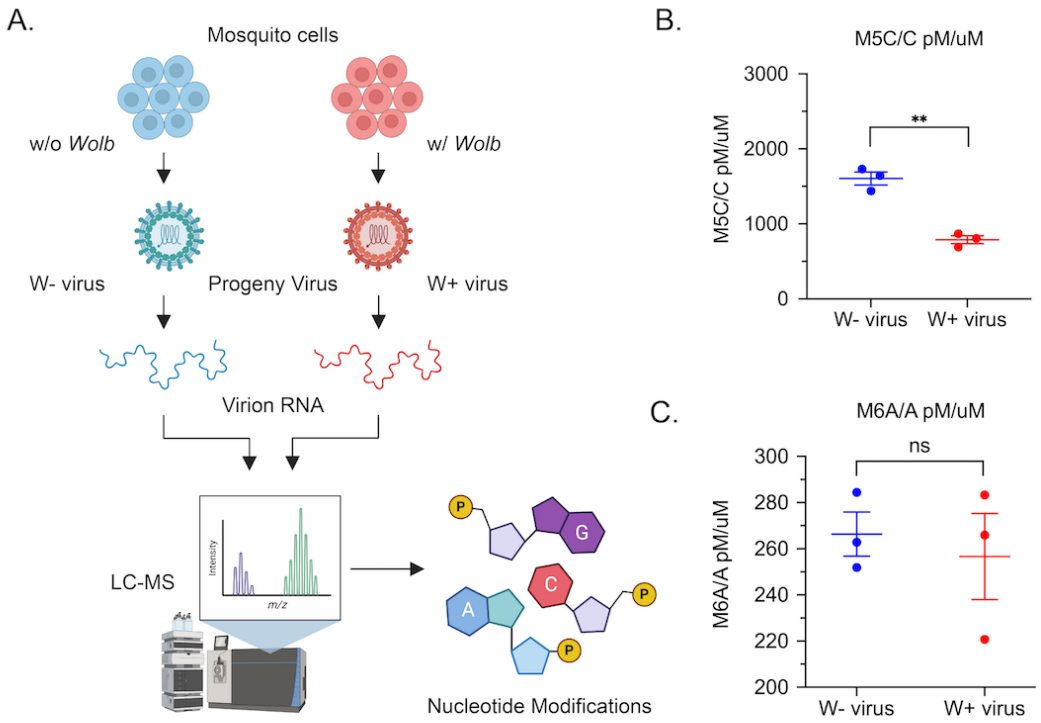

Figure 5: Presence of *Wolbachia* is associated with altered virion RNA methylation. (A) RNA isolated from progeny viruses derived from mosquito cells colonized with (W+ virus) or without (W- virus) *Wolbachia* were subjected to LC-MS/MS analyses to determine their nucleotide content. (B) Normalized 5-methyl cytosine (M5C) content of RNA isolated from W- and W+ viruses represented as a ratio of total unmodified cytosine content. (C) Normalized 6-methyl adenosine (M6A) content of RNA isolated from W- and W+ viruses represented as a ratio of total unmodified adenosine content. Error bars represent standard error of mean (SEM) of three independent virus preps from each cell type. **P < 0.01; ns = not-significant.